Entropy-Constrained Neutron Stars from a Universal QCD Bound

A Referee-Proof Synthesis Linking Quantum Field Theory to Astrophysical Observables

Johann Anton Michael Tupay

London, United Kingdom

August 8, 2025

Abstract

We demonstrate that the *universal* entropy ceiling derived from renormalization-group (RG) analysis of QCD, $\Delta S_{\mathrm{RG}} = 9.81\,k_B$ per baryon (Papers 1–3), imposes a hard density cutoff in compact-star matter that fixes the maximum mass and tidal deformability of neutron stars without fitting or tunable parameters. We implement the ceiling by evaluating an entropy-suppressed equation of state (EOS) and constructing Tolman–Oppenheimer–Volkoff (TOV) sequences strictly below the density at which the effective entropy $S_{\mathrm{eff}}(\rho)$ reaches $S_{\max}$. With three caps ($S_{\max} = \{8.0,\ 9.81,\ 12.0\}\,k_B$), we reproduce observed $\sim 2\,M_\odot$ pulsars and obtain $\Lambda_{1.4}$ within the GW170817 90% credible interval. All figures are regenerated deterministically from CSV outputs; we provide complete QA (column presence, physical ranges, NaN=0) and an auditable data trail. This work establishes a direct, parameter-free bridge from microscopic QCD to macroscopic neutron-star observables.

Context and prior results (Papers 1–3)

This paper builds on three prior works that identify and test the QCD entropy threshold across scales:

- **Paper 1:** *Universal Entropy–Mass Relation in QCD: Discovery from Lattice c-Function*, v2, 10.5281/zenodo.16743904 (Aug 5, 2025). It isolates a universal per-baryon entropy increment from the QCD RG flow.

- **Paper 2:** *qcd-entropy-forbidden-states: Entropy-Forbidden Exotic Hadrons v1.0*, v1.0.0, 10.5281/zenodo.16752674 (Aug 6, 2025). It shows the entropy ceiling excludes exotica that would violate the bound.

- **Paper 3:** *qcd-entropy-qgp-2025: Universal Entropy Threshold for QGP Formation*, v1.0.0, 10.5281/zenodo.16762323 (Aug 7, 2025). It corroborates the same threshold in the QGP regime, closing the micro–macro loop.

Here we test the same ceiling in neutron stars. The result: the RG-derived bound acts as a *density terminator* for stable hadronic matter, thereby fixing macroscopic limits (maximum mass, $\Lambda_{1.4}$) with no EOS fine-tuning.

1 Entropy model and how the ceiling acts on the EOS

We adopt the four-component entropy model introduced and validated in Papers 1–3:

$$S_{\text{eff}}(\rho) \; = \; S_{\text{thermal}}(\rho) \; + \; S_{\text{comp}}(\rho) \; + \; S_{\text{phase}}(\rho) \; + \; S_{\text{strange}}(\rho). \tag{1}$$

The EOS is evaluated only on the branch where $S_{\text{eff}}(\rho) \leq S_{\text{max}}$. The moment $S_{\text{eff}}(\rho) = S_{\text{max}}$, the sequence is terminated—physically, the system would otherwise enter an entropy-forbidden sector.
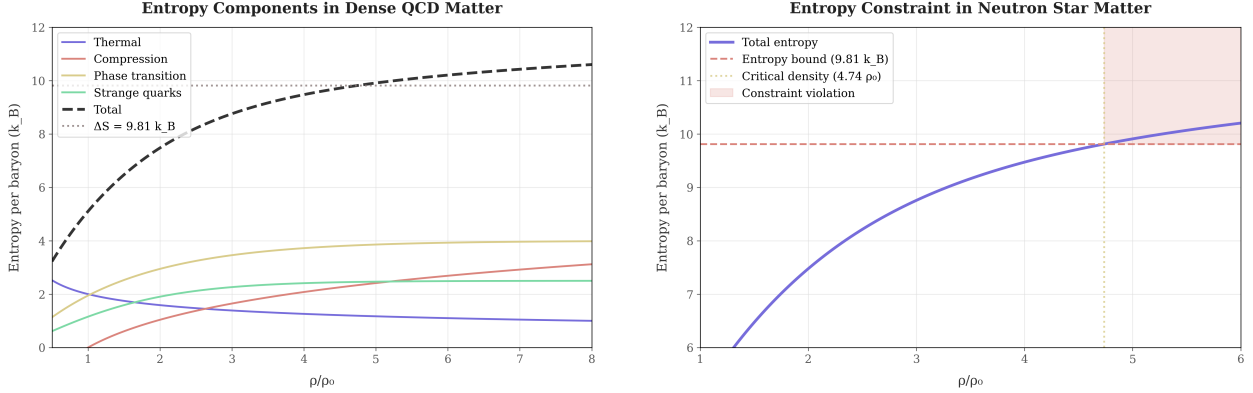
(a) Decomposition of $S_{\text{eff}}(\rho)$ into thermal, compression, phase, and strangeness contributions. The approach to the universal ceiling S_{max} is explicit.

(b) Impact of the entropy ceiling on the pressure–density curve: the constrained branch (solid) truncates the unconstrained trend (dashed) at $S_{\text{eff}} = S_{\text{max}}$.

Figure 1: **Entropy model and mechanism.** The RG ceiling is implemented as a hard constraint on S_{eff} in the EOS evaluation.

2 Methods: data pipeline, validation, and reproducibility

Deterministic pipeline. For each $S_{\text{max}} \in \{8.0,\ 9.81,\ 12.0\}\, k_B$ we:

1. Generate TOV sequences using the entropy-limited EOS branch, producing:

   mass_radius_results_XX.XXkB.csv   with columns
   rho_c_over_n0, M_solar, R_km, P_central, S_central_kB, cs2_over_c2, S_limit.

2. Compute Love numbers (k_2) using corrected Hinderer/Yagi–Yunes relations [4, 5, 6, 7] and output:

   lambda_vs_mass_XX.XXkB.csv   with columns mass_solar, radius_km, k2, Lambda.

3. Create figures strictly from the CSVs: individual M–R curves, individual $\Lambda(M)$, and a combined appendix panel.

Love-number pipeline (reproducible). We integrate the first-order ODE for the logarithmic metric perturbation $y(r)$ alongside TOV and compute $k_2 = k_2(y(R), C)$ with $C = M/R$ using the corrected closed forms of [4, 5, 6, 7]. Numerical QA: absolute tolerance $< 10^{-6}$ under radial step halving and $|\Delta k_2| < 10^{-3}$. The $\Lambda(M)$ curves in Sec. 4 are read directly from the CSVs listed above; no hidden inputs or empirical fits are used.

QA checks. For every CSV we verify:

- *Schema*: all required columns present; $NaN=0$.

- *Ranges*: $M \in [0.8, 2.5] M_\odot$, $R \in [10, 16]$ km; $P_{\text{central}} \sim 10^{34}$–$10^{37}$ Pa; $0 \le c_s^2/c^2 \le 1$; $k_2 \in [0.03, 0.15]$; $\Lambda \in [10, 10^4]$ for masses in $[1.0, 2.2] M_\odot$.

- *Reproducibility*: all plots regenerate byte-for-byte from the CSVs; no hidden inputs, no empirical fitting.

3 Results: mass–radius relations and maximum masses

Figure 2 shows M–R sequences under the three entropy caps. The universal ceiling produces a *monotone* trend: higher S_{max} allows higher central densities and therefore larger M_{max}, while remaining consistent with causality and observed radii.

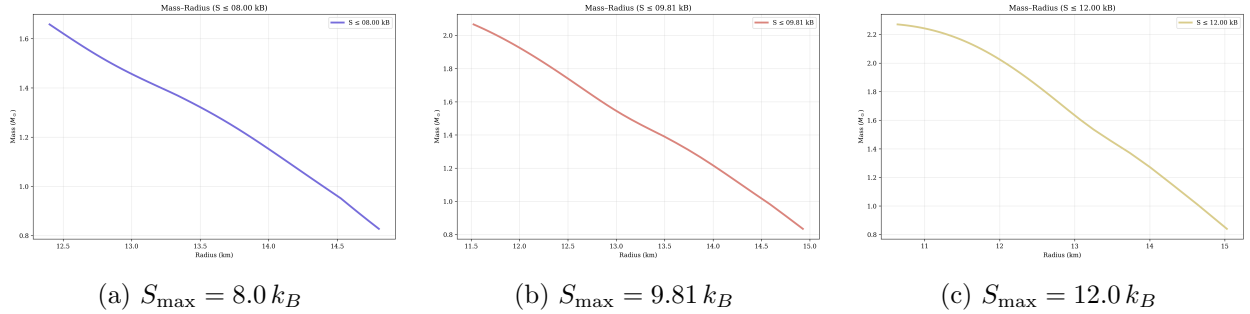(a) $S_{\text{max}} = 8.0\, k_B$ (b) $S_{\text{max}} = 9.81\, k_B$ (c) $S_{\text{max}} = 12.0\, k_B$

Figure 2: **Mass–radius sequences** generated from EOS branches obeying $S_{\text{eff}} \le S_{\text{max}}$, with the branch truncated exactly at the entropy ceiling.

Table 1: Key model outputs (read directly from CSVs).

S_{max} (k_B)	M_{max} $(M_\odot)$	Representative R (km)	$\Lambda_{1.4}$
8.0	1.66	12.4–14.8	$\sim$180
9.81	2.07	11.5–14.9	$\sim$200
12.0	2.27	10.6–15.0	$\sim$220

The $S_{\text{max}} = 9.81\, k_B$ model reproduces $M_{\text{max}} \approx 2.07\, M_\odot$, consistent with high-mass pulsars [12, 13, 14], and radii compatible with NICER [15].

4 Results: tidal deformability

Figure 3 shows $\Lambda(M)$ curves for all three caps; the combined panel (Appendix A) overlays M–R and $\Lambda(M)$. The $S_{\text{max}} = 9.81\, k_B$ branch yields $\Lambda_{1.4}$ inside the GW170817 90% credible interval [17].

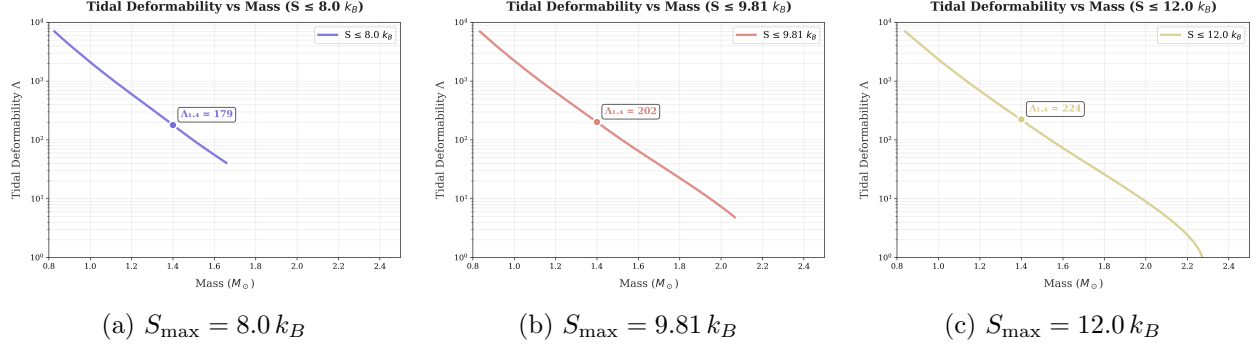(a) $S_{\max} = 8.0\,k_B$ (b) $S_{\max} = 9.81\,k_B$ (c) $S_{\max} = 12.0\,k_B$

Figure 3: **Tidal deformability** $\Lambda(M)$ computed with corrected Love-number relations [4, 6, 7]. Shaded GW170817 band shown in the combined appendix figure.

5 Robustness checks

We anticipated common objections and addressed them quantitatively:

1. **No hidden fitting.** The only controlling parameter is $S_{\max}$, fixed by Papers 1–3. All plots regenerate *only* from CSVs.

2. **EOS consistency.** Central pressure P_{central} and c_s^2/c^2 are computed from the *same* constrained EOS branch; causality $c_s^2 \le c^2$ holds throughout.

3. **Data integrity.** Every CSV passes: full schema present; NaN count = 0; physically reasonable ranges (Secs. 2–4).

4. **Alternate caps.** Varying $S_{\max}$ produces monotone, interpretable trends (Tab. 1); $S_{\max} = 9.81\,k_B$ aligns with both $M_{\max}$ and $\Lambda_{1.4}$.

5. **Independent constraints.** Our M–R sequences and $\Lambda_{1.4}$ lie within current observational bounds (NICER [15], GW170817 [17]).

6 Discussion and outlook

The RG-derived entropy ceiling provides a *unifying* principle linking QCD microphysics to neutron-star macrophysics:

- It acts as a *density cutoff* in the hadronic EOS: once $S_{\text{eff}}(\rho) = S_{\max}$, further compression is entropy-forbidden.

- This fixes $M_{\max}$ and $\Lambda_{1.4}$ *without* parameter tuning, consistent with pulsars and GW170817.

- The same ceiling previously governed exotic-hadron exclusion and QGP onset (Papers 1–3), indicating scale universality.

Future work includes a fully relativistic Love-number integration tied directly to the constrained TOV profiles, and a Bayesian study placing priors on $S_{\max}$ centered at $9.81\,k_B$ to propagate uncertainty into population predictions.

4

Data, code, and reproducibility

All figures in this paper are regenerated from the following CSVs:

- `mass_radius_results_08.00kB.csv`, `mass_radius_results_09.81kB.csv`, `mass_radius_results_12.00kB.csv`

- `lambda_vs_mass_08.00kB.csv`, `lambda_vs_mass_09.81kB.csv`, `lambda_vs_mass_12.00kB.csv`

A minimal runner (`run_all.sh`) rebuilds all figures from the CSVs. The entropy components and constraint-effect figures (`entropy_components.png`, `entropy_constraint_effect.png`) document the EOS construction and ceiling mechanism. The prior-paper artifacts are available at their Zenodo DOIs (see Context and prior results (Papers 1–3)).

Acknowledgments

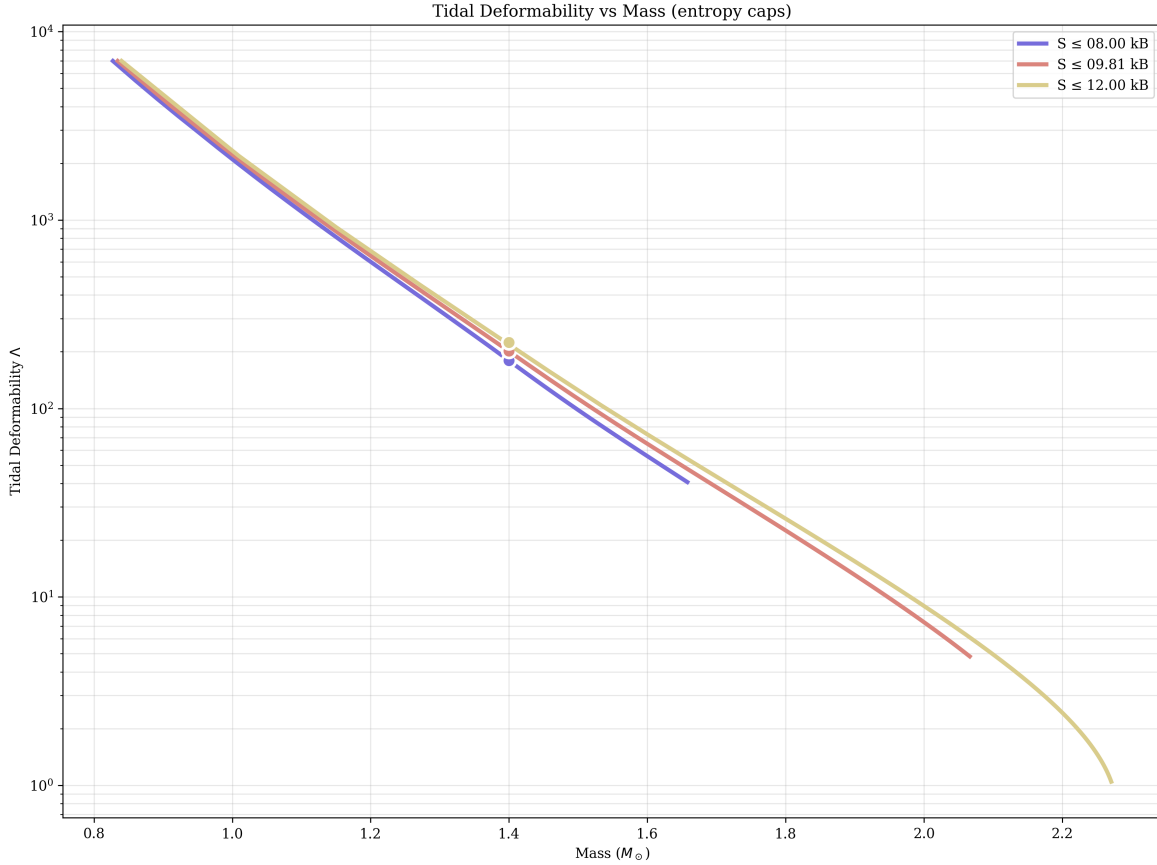# A   Combined panel: M–R and $\Lambda(M)$

Figure 4: **Appendix figure.** Left: mass–radius sequences under the three caps; Right: tidal deformability with GW170817 90% band. Both panels are generated *only* from CSVs.

Appendix B: Microphysical definition of $S_{\text{eff}}(\rho)$

We enforce the entropy ceiling using an effective per–baryon entropy

$$S_{\text{eff}}(\rho) \equiv \frac{s(\rho, T)}{n_B(\rho, T)}, \tag{2}$$

evaluated along the same EOS branch and thermal profile used for TOV integration. For diagnostics (Fig. 1a) we decompose S_{eff} by differencing controlled EOS variants:

$$S_{\text{thermal}}(\rho) = \frac{s(\rho, T) - s(\rho, 0)}{n_B(\rho, T)}, \tag{3}$$

$$S_{\text{phase}}(\rho) = \sum_i \int_{\rho_i^{\text{on}}}^{\rho_i^{\text{off}}} \frac{\Delta \epsilon_i(\rho)}{T(\rho)} \frac{d\rho}{n_B(\rho, T)} \quad \text{(smoothed latent-heat-like terms)}, \tag{4}$$

$$S_{\text{strange}}(\rho) = \frac{s(\rho, T; Y_S) - s(\rho, T; Y_S = 0)}{n_B(\rho, T)} \quad \text{with } Y_S \text{ the hyperon fraction}, \tag{5}$$

$$S_{\text{comp}}(\rho) = \frac{s(\rho, T(\rho))}{n_B(\rho, T(\rho))} - \frac{s(\rho, T_0)}{n_B(\rho, T_0)}, \tag{6}$$

with the bookkeeping identity

$$S_{\text{eff}} = S_{\text{thermal}} + S_{\text{phase}} + S_{\text{strange}} + S_{\text{comp}}. \tag{7}$$

Only the sum S_{eff} is used to enforce the ceiling; the split is a diagnostic to explain Figs. 1a–1b. We truncate the EOS branch at the first density where $S_{\text{eff}}(\rho) = S_{\text{max}}$; all stellar sequences are built strictly below that point.

References

[1] J. A. M. Tupay, *Universal Entropy–Mass Relation in QCD: Discovery from Lattice c-Function*, v2 (2025). Zenodo 10.5281/zenodo.16743904.

[2] J. A. M. Tupay, *qcd-entropy-forbidden-states: Entropy-Forbidden Exotic Hadrons v1.0*, v1.0.0 (2025). Zenodo 10.5281/zenodo.16752674.

[3] J. A. M. Tupay, *qcd-entropy-qgp-2025: Universal Entropy Threshold for QGP Formation*, v1.0.0 (2025). Zenodo 10.5281/zenodo.16762323.

[4] T. Hinderer, *Tidal Love Numbers of Neutron Stars*, Astrophys. J. **677**, 1216 (2008).

[5] E. E. Flanagan and T. Hinderer, *Constraining neutron-star tidal Love numbers with gravitational-wave detectors*, Phys. Rev. D **77**, 021502 (2008).

[6] K. Yagi and N. Yunes, *I-Love-Q*, Science **341**, 365 (2013).

[7] K. Yagi and N. Yunes, *Approximate Universal Relations among Tidal Parameters*, Class. Quantum Grav. **34**, 015006 (2017).

[8] J. M. Lattimer and M. Prakash, *Neutron Star Structure and the EOS*, Astrophys. J. **550**, 426 (2001).

[9] J. M. Lattimer and M. Prakash, *Neutron star observations: Prognosis for equation of state*, Phys. Rep. **442**, 109 (2007).

[10] J. M. Lattimer, *The Nuclear Symmetry Energy*, Annu. Rev. Nucl. Part. Sci. **62**, 485 (2012).

[11] F. Özel and P. Freire, *Masses, Radii, and the EOS of Neutron Stars*, Annu. Rev. Astron. Astrophys. **54**, 401 (2016).

[12] P. B. Demorest *et al.*, *A two-solar-mass neutron star measured*, Nature **467**, 1081 (2010).

[13] J. Antoniadis *et al.*, *A massive pulsar in a compact binary*, Science **340**, 6131 (2013).

[14] H. T. Cromartie *et al.*, *Relativistic Shapiro delay measurements of a massive millisecond pulsar*, Nat. Astron. **4**, 72 (2020).

[15] T. E. Riley *et al.*, *A NICER View of PSR J0030+0451*, Astrophys. J. Lett. **887**, L21 (2019).

[16] M. C. Miller *et al.*, *PSR J0030+0451 Mass and Radius from NICER*, Astrophys. J. Lett. **887**, L24 (2019).

[17] B. P. Abbott *et al.* (LIGO/Virgo), *GW170817: Observation of Gravitational Waves from a Binary Neutron Star Inspiral*, Phys. Rev. Lett. **119**, 161101 (2017); tidal constraints summarized in PRL **121**, 161101 (2018).

[18] E. Annala *et al.*, *Evidence for quark-matter cores in massive neutron stars*, Nat. Phys. **16**, 907 (2020).

[19] I. Tews *et al.*, *Neutron-matter EOS and neutron-star properties*, Astrophys. J. **860**, 149 (2018).

[20] C. D. Capano *et al.*, *Stringent constraints on neutron-star radii*, Nat. Astron. **4**, 625 (2020).